

층상 페로브스카이트 구조인 $\text{La}_{0.5}\text{Sr}_{1.5}\text{Mn}_{0.5}\text{Cr}_{0.5-x}\text{Fe}_x\text{O}_4$ ($x=0.15, 0.3$) 망가나이트의 구조적, 전기적, 자기적 특성의 연구

Devinder Singh*

Department of Chemistry, University of Jammu, Jammu 180006, India
(접수 2011. 5. 20; 수정 2011. 6. 24; 게재확정 2011. 6. 30)

Investigation on the Structural, Electrical and Magnetic Properties of Layered Perovskite Manganite $\text{La}_{0.5}\text{Sr}_{1.5}\text{Mn}_{0.5}\text{Cr}_{0.5-x}\text{Fe}_x\text{O}_4$ ($x=0.15, 0.3$) System

Devinder Singh*

Department of Chemistry, University of Jammu, Jammu 180006, India.
*E-mail address: drdssambyal@rediffmail.com

(Received May 20, 2011; Revised June 24, 2011; Accepted June 30, 2011)

요 약. 새로운 층상구조인 페로브스카이트 망가나이트 $\text{La}_{0.5}\text{Sr}_{1.5}\text{Mn}_{0.5}\text{Cr}_{0.5-x}\text{Fe}_x\text{O}_4$ ($x=0.15, 0.3$) 를 세라믹 방법에 의해 합성하였다. 분말 X-선 측정을 통하여 $I4/mmm$ 의 정방정계 단위세포를 확인하였다. 전기전도도 측정을 통하여 부도체의 특성을 확인하였으며 전기전도도는 3D 홉핑 메커니즘에 의해 나타난다. 자기적 특성은 모두 반강자성의 특성을 보인다.

주제어: 층상 페로브스카이트 산화물, 페로브스카이트 망가나이트, 전기전도도, 자기적 특성

ABSTRACT. The new layered perovskite manganites $\text{La}_{0.5}\text{Sr}_{1.5}\text{Mn}_{0.5}\text{Cr}_{0.5-x}\text{Fe}_x\text{O}_4$ ($x=0.15, 0.3$) have been prepared by standard ceramic method. The powder X-ray diffraction studies show that the phases crystallize with tetragonal unit cell in the space group $I4/mmm$. The electrical transport properties suggest that the phases show insulating behaviour and the electrical conduction in the phases occurs by a 3D variable range hopping mechanism. The magnetic properties suggest that both the phases are antiferromagnetic.

Keywords: Layered perovskite oxides, Perovskite manganites, Electrical properties, Magnetic properties

INTRODUCTION

Layered perovskite oxides are a promising group of mixed-conducting materials with potential applications for oxygen-separation membranes, gas sensor devices and electrodes of intermediate-temperature solid oxide fuel cells.¹⁻⁴ In general, the layered perovskite can be represented as Ruddlesden-Popper (RP) series of general formula $\text{A}_{n+1}\text{B}_n\text{O}_{3n+1}$ or $\text{AO} \cdot (\text{ABO}_3)_n$, where A is an alkaline earth/rare earth ion and B is a transition metal ion. These phases generally crystallize with tetragonal or orthorhombic unit cell in the space group $I4/mmm$ or $Fmmm$ and are antiferromagnetic electrical insulators in physical behaviour.⁵⁻⁸ The crystal structure of RP phases can be described by the stacking of finite n layers of perovskite ABO_3 between rock salt AO layers along the crystallographic c direction.^{9,10} The corner-sharing BO_6 octahedra form infinite sheets in the ab plane where strong electronic interactions can occur. The $n=1$ member of this series (A_2BO_4)

exhibits a quasi-two-dimensional K_2NiF_4 -type structure (Fig. 1), with only one layer of corner sharing BO_6 octahedra along the c direction. The nature of A and B ions plays an important role in determining their physical properties. In many cases, more than one ions have been added at the sites A and B to look for novel physical properties such as electric transport and magnetic behaviour.¹¹⁻¹³

In the past few years, the layered manganites $\text{La}_{2-2x}\text{Sr}_{1+2x}\text{Mn}_2\text{O}_7$ of Ruddlesden-Popper phases ($n=2$) attracted considerable attention due to their novel physical properties such as the colossal magnetoresistance effect, the tunneling magnetoresistance and fascinating magnetic properties because of mixed valence of manganese.¹⁴⁻¹⁶ It is well known that the correlation between the magnetic and electrical properties in the mixed-valence manganites is generally understood in terms of the double exchange (DE) interaction mechanism.¹⁷ Besides the DE mechanism, the Jahn-Teller effect, phase separation (PS)¹⁸ and antiferromagnetic (AFM) superexchange and charge-orbital

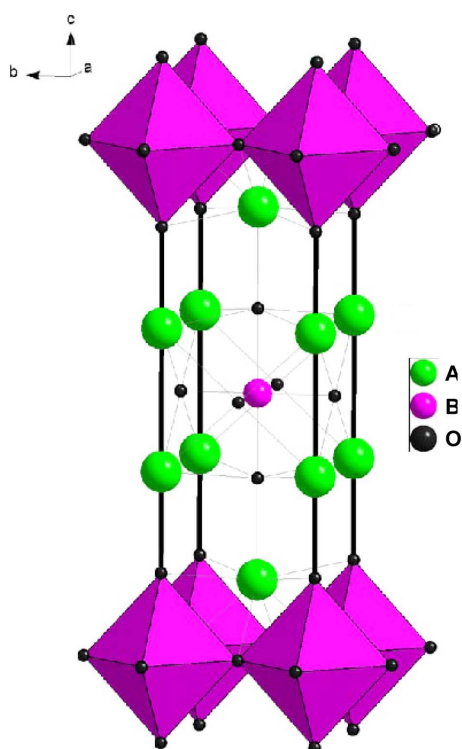


Fig. 1. Structure of A_2BO_4 (K_2NiF_4 -Type).

ordering interactions also play an important role. In order to get further understanding of this mechanism, Mn-site doping in the layered manganites can dramatically change the magnetic and electrical properties. Some such studies have been undertaken during the past few years.¹⁹⁻²⁵ Cr and Fe are very interesting substitution ions for Mn site. The choice of Cr^{3+} is based on the fact that its electronic structure is same as that of Mn^{4+} and its ionic radius (0.62\AA) is smaller than that of the Mn^{3+} (0.65\AA). For the Fe^{3+} ion, its ionic radius is close the Mn^{3+} ionic radius.²⁶ Fe and Cr are the nearest neighbors of Mn in the periodic table and they are non-Jahn-Teller ions. Some reports on the effect of Cr and Fe doping in the cubic perovskite manganites have appeared, and several reports on such studies have also appeared in case of bilayered manganites.²⁷⁻³¹ Some authors have proposed that there may be ferromagnetic (FM) DE interaction between Cr^{3+} and Mn^{3+} just as between Mn^{4+} and Mn^{3+} . On the other hand, the Fe^{3+} ion is usually unable to participate in the double exchange interaction—the ferromagnetic interactions $Mn^{4+}-O-Mn^{3+}$ are destroyed and replaced by antiferromagnetic $Mn^{4+}-O-Fe^{3+}$ interactions, which lead to a progressive dilution of ferromagnetism.³²⁻³⁶ Because of this, Fe and Cr dopings on the Mn site are expected to show interesting physical properties and should provide useful information for the

understanding of the physical mechanisms in layered manganites.

In the present work, two new RP type $n=1$ manganites $La_{0.5}Sr_{1.5}Mn_{0.5}Cr_{0.5-x}Fe_xO_4$ ($x=0.15, 0.3$) have been synthesized by standard ceramic method where two/three ions are substituted at A and B sites to look for novel physical properties. Their crystal structure has been determined by powder X-ray diffractometry. The electric transport and magnetic properties have been studied as a function of temperature.

EXPERIMENTAL

The samples of $La_{0.5}Sr_{1.5}Mn_{0.5}Cr_{0.35}Fe_{0.15}O_4$ and $La_{0.5}Sr_{1.5}Mn_{0.5}Cr_{0.2}Fe_{0.3}O_4$ were synthesized by the following procedure. The powders of La_2O_3 (Aldrich 99.9%), MnO_2 (Aldrich 99.9%), Cr_2O_3 (Aldrich 99.9%), Fe_2O_3 (Aldrich 99.9%) and $SrCO_3$ (Aldrich 99.9%) were weighed in the ratios corresponding to the stoichiometry of the desired phases. Prior to use, La_2O_3 was heated at $1000\text{ }^\circ\text{C}$ to remove moisture. The powders were mixed and homogenized by grinding with an alumina mortar and pestle. The mixtures were then pressed into pellets 10 mm in diameter and 1 mm thick by hydraulic press under 20 MPa, and then calcined at 1200 K in static air atmosphere in an electric tube furnace for about 36 hours. The calcined pellets were ground, and again pressed into pellets by hydraulic press under 20 MPa, and then calcined at 1563 K for about 72 hours in static air atmosphere with a number of intermediate grindings and pelletizings. The samples were then cooled down slowly to room temperature in the electric furnace.

Room temperature X-ray diffraction data of the phases were recorded on Bruker AXS diffractometer-D8 (D76181 Karlsruhe, Germany) using CuK_α radiations at a scanning speed of $1^\circ/\text{minute}$. The experimental XRD data are given in Tables 1 and 2, while the pattern is plotted in Fig. 2. The total amount of various constituent cations was estimated by Perkin Elmer atomic absorption spectrometer 700. The oxygen content in the samples was determined by modified iodometric technique within error limits of ± 0.01 . The samples were dissolved in concentrated HCl and the resulted chlorine was absorbed by a KI solution. The titration was made by using 0.005 N standard sodium thiosulphate solution. The details of the method have been described elsewhere.³⁷ The precise chemical composition of the phases was determined to be $La_{0.5}Sr_{1.5}Mn_{0.5}Cr_{0.35}Fe_{0.15}O_{3.981}$ and $La_{0.5}Sr_{1.5}Mn_{0.5}Cr_{0.2}Fe_{0.3}O_{3.984}$.

The electrical resistivity of the sintered pellets of the

Table 1. Powder X-ray diffraction data of $\text{La}_{0.5}\text{Sr}_{1.5}\text{Mn}_{0.5}\text{Cr}_{0.35}\text{Fe}_{0.15}\text{O}_4$ (Space group: $I4/mmm$) [$a=3.8679(3)$ Å; $c=12.6714(3)$ Å]

h	k	l	$d_{\text{obs}}(\text{Å})$	$d_{\text{cal}}(\text{Å})$	I_{obs}	I_{cal}
0	0	2	6.333	6.331	19	28
1	0	1	3.694	3.696	26	24
0	0	4	3.167	3.165	22	27
1	0	3	2.846	2.850	100	100
1	1	0	2.732	2.733	87	83
1	0	5	2.115	2.118	23	30
1	1	4	2.068	2.069	37	46
2	0	0	1.931	1.932	39	55
1	1	6	1.668	1.670	16	34
1	0	7	1.639	1.638	15	18
2	1	3	1.598	1.599	31	46
0	0	8	1.584	1.583	21	14
2	1	5	1.425	1.427	17	18
2	2	0	1.371	1.366	16	23
3	1	0	1.221	1.222	15	19

Table 2. Powder X-ray diffraction data of $\text{La}_{0.5}\text{Sr}_{1.5}\text{Mn}_{0.5}\text{Cr}_{0.2}\text{Fe}_{0.3}\text{O}_4$ (Space group: $I4/mmm$) [$a=3.8763(3)$ Å; $c=12.6737(3)$ Å]

h	k	l	$d_{\text{obs}}(\text{Å})$	$d_{\text{cal}}(\text{Å})$	I_{obs}	I_{cal}
0	0	2	6.348	6.332	20	28
1	0	1	3.696	3.704	21	24
0	0	4	3.177	3.166	18	27
1	0	3	2.851	2.854	100	100
1	1	0	2.739	2.739	73	83
1	0	5	2.120	2.120	24	29
1	1	4	2.070	2.071	29	46
2	0	0	1.937	1.937	41	55
1	1	6	1.672	1.672	16	34
1	0	7	1.645	1.645	15	17
2	1	3	1.598	1.602	26	46
0	0	8	1.584	1.583	27	14
2	1	5	1.427	1.430	19	17
2	2	0	1.370	1.369	20	24
3	1	0	1.227	1.225	18	21

phases was measured by four probe method in the temperature range 150-300 K. Thin copper wires were attached to the surface of pellets with silver paste for the purpose of electrodes. The magnetic susceptibility of the powdered samples was measured by Faraday magnetic balance under constant magnetic field of 3,700 gauss in the temperature range 100-300 K. The magnetic susceptibility of the samples was calculated after diamagnetic correction for the constituent ions in the phase.

RESULTS AND DISCUSSION

All the peaks of X-ray diffraction pattern of polycrys-

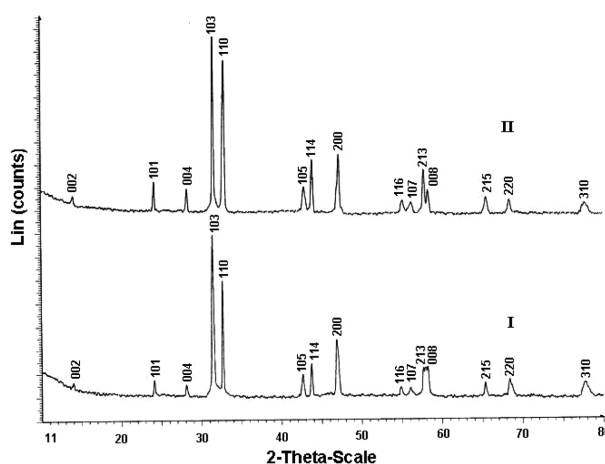


Fig. 2. X-ray diffraction patterns of $\text{La}_{0.5}\text{Sr}_{1.5}\text{Mn}_{0.5}\text{Cr}_{0.2}\text{Fe}_{0.3}\text{O}_4$ (I) and $\text{La}_{0.5}\text{Sr}_{1.5}\text{Mn}_{0.5}\text{Cr}_{0.35}\text{Fe}_{0.15}\text{O}_4$ (II).

talline samples were successfully indexed on the tetragonal unit cell in the space group $I4/mmm$. The unit cell parameters and space group were determined and tested by using program “*Checkcell*”³⁸ and are listed in the *Tables 1 and 2*. The atomic positions of La/Sr, Mn/Cr/Fe and O for $\text{La}_{0.5}\text{Sr}_{1.5}\text{Mn}_{0.5}\text{Cr}_{0.35}\text{Fe}_{0.15}\text{O}_4$ and $\text{La}_{0.5}\text{Sr}_{1.5}\text{Mn}_{0.5}\text{Cr}_{0.2}\text{Fe}_{0.3}\text{O}_4$ have been estimated from analogy with Sr_2VO_4 without refinement.³⁹ The theoretical diffraction intensities of the phases (*Tables 1 and 2*) were determined by using programs “*Diamond*” (Method of Klaus Brandenburg 1998) and “*Mercury 2.3*” based on the atomic positions, cell parameters and space group $I4/mmm$. The agreement between the experimental and theoretical intensities is in general satisfactory considering that atomic positions are not refined and that any preferred orientation effects are neglected. The XRD results confirmed the formation of RP type ($n=1$) $\text{La}_{0.5}\text{Sr}_{1.5}\text{Mn}_{0.5}\text{Cr}_{0.35}\text{Fe}_{0.15}\text{O}_4$ and $\text{La}_{0.5}\text{Sr}_{1.5}\text{Mn}_{0.5}\text{Cr}_{0.2}\text{Fe}_{0.3}\text{O}_4$ phases.

Analysis of the cell parameters shows that increase in iron content leads to slight increase in c parameter while the corresponding increase in a parameter is much larger. In particular a would be expected to be affected by the transition metal as the perovskite slabs in the K_2NiF_4 -type structure linked through corner sharing in the ab plane. The c axis, on the other hand, should be strongly dominated by the La/Sr-O bonds. The partial replacement of Cr^{3+} (ionic radius=0.62Å) by larger Fe^{3+} (ionic radius=0.65Å) might therefore be expected to increase cell parameter a more significantly than c .

The temperature dependence of electrical resistivity is given in *Fig. 3*, where $\log \rho$ is plotted against temperature (T). The plot shows that the temperature coefficient of

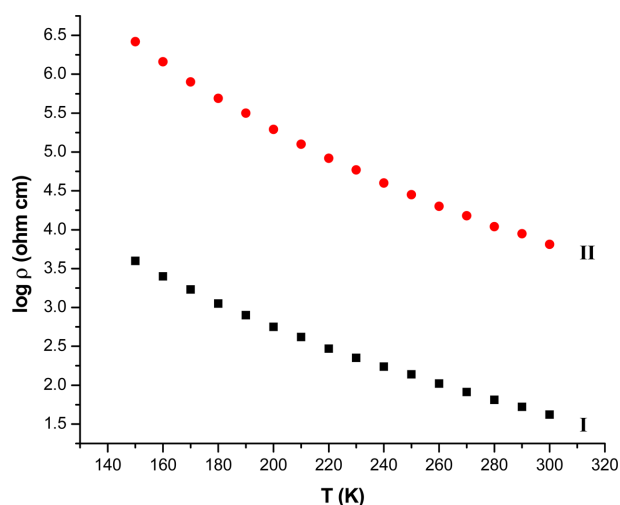


Fig. 3. Plots of $\log \rho$ versus Temperature (K) for $\text{La}_{0.5}\text{Sr}_{1.5}\text{Mn}_{0.5}\text{Cr}_{0.2}\text{Fe}_{0.3}\text{O}_4$ (I) and $\text{La}_{0.5}\text{Sr}_{1.5}\text{Mn}_{0.5}\text{Cr}_{0.35}\text{Fe}_{0.15}\text{O}_4$ (II).

resistivity of both the phases is negative suggesting that materials are insulators in the temperature range 150-300K. The insulator behavior in both the phases is attributed to the super exchange coupling of electrons. The similar results have also been reported earlier in such RP-type phases containing Mn, Fe and Cr ions at B site.⁴⁰⁻⁴² The results suggest that the electrical resistivity increases with decreasing iron content, which could be attributed to enhancement of the 3D-character along c-axis because of the coming closer of (Mn/Cr/Fe)O₂ and (La,Sr)O layers along the c-axis as a result of replacement of Fe³⁺ ion by smaller Cr³⁺ ion. Various equations based upon different mechanisms of conduction, such as those applicable in case of Arrhenius model, polaron hopping model and variable range hopping model have been applied to the data of electrical resistivity of the phases. It was observed that the equation based on variable range hopping mechanism defined by the relation, $\rho = \rho_0 \exp(BT^{-1/4})$ was applicable to the data. The linearity of plot between $\log \rho$ and $T^{-1/4}$ (Fig. 4) shows that the electrical conduction in these phases occurs by a 3D variable range hopping mechanism which is generally observed in such perovskite-related phases.^{30,42} The characteristic energy of hopping (B), calculated from the slopes of $\log \rho$ versus $T^{-1/4}$ plots, is equal to 5.5 and 3.5 K^{-1/4} for $\text{La}_{0.5}\text{Sr}_{1.5}\text{Mn}_{0.5}\text{Cr}_{0.35}\text{Fe}_{0.15}\text{O}_4$ and $\text{La}_{0.5}\text{Sr}_{1.5}\text{Mn}_{0.5}\text{Cr}_{0.2}\text{Fe}_{0.3}\text{O}_4$, respectively. The comparatively large value of B for $\text{La}_{0.5}\text{Sr}_{1.5}\text{Mn}_{0.5}\text{Cr}_{0.35}\text{Fe}_{0.15}\text{O}_4$ phase suggests that insulator behavior is more pronounced in this phase.

The temperature dependence of inverse molar magnetic susceptibility is shown in Fig. 5. Linearity of plots shows that the Curie-Weiss law is followed in the tem-

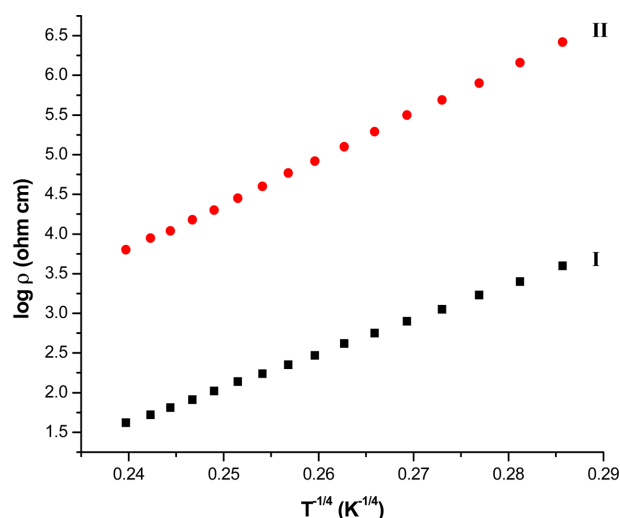


Fig. 4. Plots of $\log \rho$ versus $T^{-1/4}$ for $\text{La}_{0.5}\text{Sr}_{1.5}\text{Mn}_{0.5}\text{Cr}_{0.2}\text{Fe}_{0.3}\text{O}_4$ (I) and $\text{La}_{0.5}\text{Sr}_{1.5}\text{Mn}_{0.5}\text{Cr}_{0.35}\text{Fe}_{0.15}\text{O}_4$ (II).

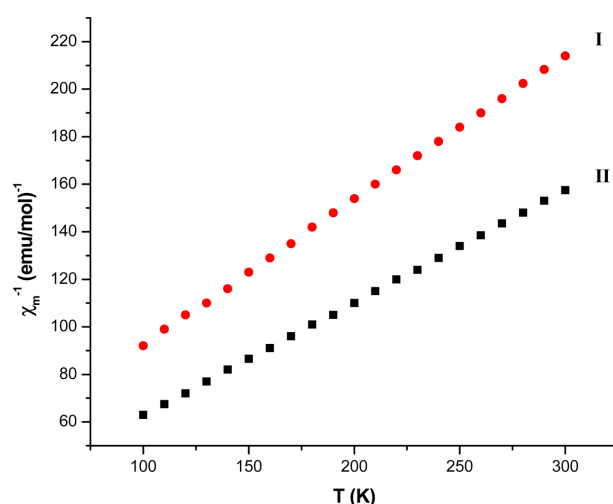


Fig. 5. Plots of Inverse molar susceptibility (χ_m^{-1}) versus Temperature (K) for $\text{La}_{0.5}\text{Sr}_{1.5}\text{Mn}_{0.5}\text{Cr}_{0.2}\text{Fe}_{0.3}\text{O}_4$ (I) and $\text{La}_{0.5}\text{Sr}_{1.5}\text{Mn}_{0.5}\text{Cr}_{0.35}\text{Fe}_{0.15}\text{O}_4$ (II).

perature range of investigation. The Weiss constant (θ) is negative for both the phases suggesting that magnetic interactions are antiferromagnetic. The values of effective magnetic moment (μ_{eff}) estimated from the slope of χ_m^{-1} versus T plot comes out to be 4.14 and 3.63 B. M. for $\text{La}_{0.5}\text{Sr}_{1.5}\text{Mn}_{0.5}\text{Cr}_{0.35}\text{Fe}_{0.15}\text{O}_4$ and $\text{La}_{0.5}\text{Sr}_{1.5}\text{Mn}_{0.5}\text{Cr}_{0.2}\text{Fe}_{0.3}\text{O}_4$, respectively. The theoretical spin only magnetic moment has been calculated from the relationship⁴³

$$\mu_{\text{cal}} = \sqrt{X_1\mu_1^2 + X_2\mu_2^2 + X_3\mu_3^2 + X_4\mu_4^2}$$

where μ_1 , μ_2 , μ_3 and μ_4 are the theoretical magnetic moments of high spin Mn³⁺, Mn⁴⁺, Cr³⁺, and Fe³⁺ ions and X_1 , X_2 , X_3 and X_4 are their relative molar fractions. The μ_{cal} values for $\text{La}_{0.5}\text{Sr}_{1.5}(\text{Mn}_{0.462}^{4+}\text{Mn}_{0.038}^{3+})\text{Cr}_{0.35}\text{Fe}_{0.15}\text{O}_{3.981}$ and

$\text{La}_{0.5}\text{Sr}_{1.5}(\text{Mn}_{0.468}^{4+}\text{Mn}_{0.032}^{3+})\text{Cr}_{0.2}\text{Fe}_{0.3}\text{O}_{3.984}$ comes to be 4.28 and 4.61 B.M., respectively. The decrease in μ_{eff} value compared to spin only μ_{cal} value in both the phases is attributed to antiferromagnetic interactions. The similar results have also been reported earlier in such RP-type phases.^{8,40-42} Generally, the magnetic interaction between Cr^{3+} and Mn^{3+} is FM, and that between Cr^{3+} and Mn^{4+} is AFM.^{31,44} Furthermore, the Fe^{3+} ions do not participate in the double exchange interaction with the Mn^{4+} ions.³³ Thus, the antiferromagnetic behaviour of the phases could be due to the antiferromagnetic interactions of the type $\text{Mn}^{4+}\text{-O-Mn}^{4+}$, $\text{Mn}^{4+}\text{-O-Cr}^{3+}$, $\text{Mn}^{4+}\text{-O-Fe}^{3+}$, $\text{Fe}^{3+}\text{-O-Mn}^{3+}$, $\text{Cr}^{3+}\text{-O-Cr}^{3+}$ and $\text{Fe}^{3+}\text{-O-Fe}^{3+}$. As the stoichiometry of the phases indicates the presences of some Mn^{3+} ions, there might be some ferromagnetic interactions of the type $\text{Mn}^{3+}\text{-O-Mn}^{4+}$ and $\text{Cr}^{3+}\text{-O-Mn}^{3+}$ but the antiferromagnetic interactions predominates over ferromagnetic interactions because of much higher concentration of Mn^{4+} compared to Mn^{3+} ions which results in the antiferromagnetic behaviour of the phases.

CONCLUSIONS

The RP-type phases $\text{La}_{0.5}\text{Sr}_{1.5}\text{Mn}_{0.5}\text{Cr}_{0.35}\text{Fe}_{0.15}\text{O}_4$ and $\text{La}_{0.5}\text{Sr}_{1.5}\text{Mn}_{0.5}\text{Cr}_{0.2}\text{Fe}_{0.3}\text{O}_4$, prepared by ceramic method, crystallize with tetragonal unit cell in the space group $I4/mmm$. The increase in unit cell volume by the replacement of Cr by Fe is in accordance with ionic sizes of the two. The Weiss constant (θ) suggests that both phases are antiferromagnetic. The electrical conduction in both the phases occurs by variable range hopping mechanism.

Acknowledgements. Thanks are due to Prof. A. Ramanan, Department of Chemistry, Indian Institute of Technology, New Delhi, for providing computer programmes for structure determination and Prof. Ramesh Chandra, Institute Instrumentation Centre, Indian Institute of Technology, Roorkee, for recording XRD data.

REFERENCES

- Moseley, P. T.; Williams, D. E. *Polyhedron* **1989**, *9*, 1615.
- Meixner, H.; Lampe, U. *Sensors and Actuators B* **1996**, *33*, 198.
- Skinner, S. J.; Kilner, J. A. *Solid State Ion.* **2000**, *135*, 709.
- Ormerod, R. M. *Chem. Soc. Reviews* **2003**, *32*, 17.
- Rao, C. N. R.; Ganguly, P.; Singh, K. K.; Mohan Ram, R. A. *J. Solid State Chem.* **1988**, *72*, 14.
- Sreedhar, K.; McElfresh, M.; Perry, D.; Kim, D.; Metcalf, P.; Honig, J. M. *J. Solid State Chem.* **1994**, *110*, 208.
- Zhang, Z.; Greenblatt, M.; Goodenough, J. B. *J. Solid State Chem.* **1994**, *108*, 402.
- Sharma, I. B.; Singh, D. *Bull. Mater. Sci.* **1998**, *21*, 363.
- Ruddlesden, S. N.; Popper, P. *Acta Crystallogr.* **1957**, *10*, 538.
- Ruddlesden, S. N.; Popper, P. *Acta Crystallogr.* **1958**, *11*, 54.
- Kakol, Z.; Spalek, J.; Honig, J. M. *J. Solid State Chem.* **1989**, *79*, 288.
- Kim, S. H.; Battle, P. D. *J. Solid State Chem.* **1994**, *112*, 262.
- Sreedhar, K.; Honig, J. M. *J. Solid State Chem.* **1994**, *111*, 147.
- Moritomo, Y.; Asamitsu, A.; Kuwahara, H.; Tokura, Y. *Nature (London)* **1996**, *380*, 141.
- Kimura, T.; Tomioka, Y.; Kuwahara, H.; Asamitsu, A.; Tamura, M.; Tokura, Y. *Science* **1996**, *274*, 1698.
- Kimura, T.; Tokura, Y. *Annu. Mater. Sci.* **2000**, *30*, 451.
- Zener, C. *Phys. Rev.* **1951**, *82*, 403.
- Dagotto, E.; Hotta, T.; Moreo, A. *Phys. Rep.* **2001**, *344*, 1.
- Zhang, J.; Wang, F.; Zhang, P.; Yan, Q. *J. Appl. Phys.* **1999**, *86*, 1604.
- Zhu, H.; Xu, X. J.; Pi, L.; Zhang, Y. H. *Phys. Rev. B* **2000**, *62*, 6754.
- Zhu, H.; Xu, X. J.; Ruan, K. Q.; Zhang, Y. H. *Phys. Rev. B* **2002**, *65*, 104424.
- Wiegand, F.; Gold, S.; Schmid, A.; Geissier, J.; Goering, E. *Appl. Phys. Lett.* **2002**, *81*, 2035.
- Onose, Y.; He, J. P.; Kannko, Y.; Arima, T.; Tokura, Y. *Appl. Phys. Lett.* **2005**, *86*, 242502.
- Banerjee Sunil Nair, A. *Phys. Rev. B* **2004**, *70*, 104428.
- Ang, R.; Lu, W. J.; Zhang, R. L.; Zhao, B. C.; Zhu, X. B.; Song, W. H.; Sun, Y. P. *Phys. Rev. B* **2005**, *72*, 184417.
- Shannon, R. D. *Acta Crystallogr. Sect. A* **1976**, *32*, 75.
- Gundkaram, R.; Lin, J. G.; Lee, F. Y.; Tai, M. F.; Shen, C. H.; Huang, C. Y.; *J. Phys. Condens. Matter* **1999**, *11*, 5187.
- Zhang, J.; Yan, Q.; Wang, F.; Yuan, P.; Zhang, P. *J. Phys. Condens. Matter* **2000**, *12*, 1981.
- Chashka, K. B.; Fisher, B.; Genossar, J.; Keren, A.; Patlagon, L.; Reisner, G. M.; Shimshoni, E.; Mitchell, J. F. *Phys. Rev. B* **2002**, *65*, 134441.
- Zhang, R. L.; Zhao, B. C.; Song, W. H.; Ma, Y. Q.; Yang, J.; Sheng, Z. G.; Dai, J. M. *J. Appl. Phys.* **2004**, *96*, 4965.
- Matsukawa, M.; Chiba, M.; Kikuchi, E.; Suryanarayanan, R.; Apostu, M.; Nimori, S.; Sugimoto, K.; Kobayashi, N. *Phys. Rev. B* **2005**, *72*, 224422.
- Chang, Y. L.; Huang, Q.; Ong, C. K. *J. Appl. Phys.* **2002**, *91*, 789.
- Ahn, K. H.; Wu, X. W.; Liu, K.; Chien, C. I. *Phys. Rev. B* **1996**, *54*, 15299.
- Ahn, K. H.; Wu, X. W.; Liu, K.; Chien, C. I. *J. Appl. Phys.* **1999**, *81*, 5505.
- Blanco, J. J.; Insausti, M.; Gil de Muro, I.; Lezama, L.; Rojo, T. *J. Solid State Chem.* **2006**, *179*, 623.
- Laiho, R.; Lisunov, K. G.; Lahderanta, E.; Salminen, J.;

- Zakhvalinskii, V. S. *J. Magn. Magn. Mater.* **2002**, 250, 276.
37. Krogh Anderson, I. G.; Krogh Anderson, E.; Norby, P.; Skou, E. *J. Solid. State. Chem.* **1994**, 113, 320.
38. Laugier, J.; Bochu, B. *Checkcell*, programme developped dans Laboratoire des Materiaux et du Genie Physique, Ecole nationale Superieure de Physique de Grenoble (INPG) <http://www.inpg.fr/LMGP>.
39. Rey, M. J.; Dehaut, P.; Joubert, J. C.; Lambert-Andron, B.; Cyrot. M.; Cyrot-Lackmann, F. *J. Solid. State. Chem.* **1990**, 86, 101.
40. Sharma, I. B.; Singh, D. *Ind. J. Chem.* **1997**, 36A, 80.
41. Sharma, I. B.; Magotra, S. K.; Singh, D.; Batra, S.; Mudher, K. D. S. *J. Alloys Compds.* **1999**, 291, 16.
42. Singh, D.; Singh, R. *J. Chem. Sci.* **2010**, 122, 807.
43. Porta, P.; Minelli, G.; Botton, I. L.; Baran, E. J. *J. Solid State Chem.* **1991**, 92, 202.
44. Goodenough, J. B. *Magnetism and the Chemical Bond*, Interscience; New York, 1963.
-